

# Electronic excitations of polyalanine; test of the independent chromophore approximation

Eyal Goldmann,<sup>a</sup> Sanford A. Asher<sup>b</sup> and Shaul Mukamel<sup>a</sup>

<sup>a</sup> Department of Chemistry, University of Rochester, Rochester, NY 14627-0216, USA

<sup>b</sup> Department of Chemistry, University of Pittsburgh, Pittsburgh, PA 15260, USA

Received 31st January 2001, Accepted 25th April 2001

First published as an Advance Article on the web 25th June 2001

Optical spectra of polyalanine in the  $W(\pi\pi^*)$  and  $NV_1(\pi\pi^*)$  bands are calculated using the time-dependent Hartree–Fock technique and the INDO/S Hamiltonian. Examination of the transition density matrices shows that excitations in the  $NV_1$  band involve significant charge transfer between nearest and third-nearest neighbor amide groups. Our analysis suggests that the Frenkel exciton Hamiltonian cannot adequately describe the electronic excitations in the  $NV_1$  band.

## I. Introduction

Beginning nearly 50 years ago with Moffitt's analysis of polypeptides in the  $\alpha$ -helix conformation,<sup>1</sup> much effort has been devoted to developing theoretical models capable of predicting the absorption spectra of proteins of specified geometry. The most common approach to this problem is the matrix method,<sup>2</sup> in which a basis set for the electronic excitations of the polypeptide consists of states in which the constituent amide groups are singly excited. A Hamiltonian matrix is then constructed in which the diagonal elements are the single chromophore excitation energies, and the off-diagonal elements are the couplings between the single-chromophore transitions, computed from the interaction between the transition charge densities. The matrix method is formally equivalent to the Frenkel exciton model,<sup>3–5</sup> which is commonly used for describing the electronic spectra of molecular crystals and chromophore aggregates. This model is valid when orbitals on different chromophores do not overlap, and when interchromophore charge transfer does not occur during excitation.

Modeling electronic excitations with the Frenkel exciton Hamiltonian greatly simplifies the theoretical analysis and allows for the generation of all spectroscopic information using computations performed on a single chromophore unit. For that reason, Frenkel Hamiltonians are commonly used in the analysis of optical properties such as linear absorption, linear dichroism and circular dichroism (CD). Frenkel exciton studies of proteins have had a particular emphasis on constructing models which accurately predict CD spectra, since experimental CD measurements are an important tool in the analysis of protein secondary structure.<sup>6,7</sup> Despite the long history of efforts in this direction, however, only recently have theoretical studies reported near-quantitative success in predicting the CD of proteins directly from their geometric structure.<sup>8–10</sup>

In this article we put the Frenkel Hamiltonian for the  $NV_1$  band of proteins to a critical test, and address the issue of whether it is possible to dissect a polypeptide into chromophores with nonoverlapping charge distributions. We have performed collective electronic oscillator (CEO) calculations<sup>11</sup> on both a 5-amide  $\text{CH}_3-(\text{CONHC}_2\text{H}_4)_5-\text{CH}_3$  (ALA5) and a 15-amide polyalanine  $\text{CH}_3-(\text{CONHC}_2\text{H}_4)_{15}-\text{CH}_3$  (ALA15) in

the  $\alpha$ -helix configuration. The geometry of these molecules was generated by a simple repetition of the experimentally determined monomer unit.<sup>12</sup> From an analysis of the excitations of the 5-amide polyalanine, we constructed a Frenkel Hamiltonian which, *a priori*, should be applicable to arbitrary length polyalanines which share this structure. However, we found that excitation in the  $NV_1$  band involved charge transfer between amide groups and the Hamiltonian so obtained failed to reproduce even qualitative features of the  $NV_1$  band of ALA15. In the case of ALA5, charge transfer occurred primarily between neighboring groups. For ALA15 we also found charge transfer between third-nearest neighbors, as expected from the helical structure.

## II. The Frenkel-excitation model

The multiband Frenkel exciton model Hamiltonian is<sup>3–5</sup>

$$H = \sum_{v \in \alpha} \Omega_v^{(\alpha)} B_v^{(\alpha)\dagger} B_v^{(\alpha)} + \sum_{\alpha \neq \beta} \sum_{\substack{v \in \alpha \\ \mu \in \beta}} J_{v\mu}^{(\alpha\beta)} B_v^{(\alpha)\dagger} B_\mu^{(\beta)} \quad (1)$$

where  $B_v^{(\alpha)\dagger}$  takes chromophore  $\alpha$  from its ground state to its  $v$ 'th excited state,  $\Omega_v^{(\alpha)}$  is the energy of the  $v$ 'th excitation on the isolated chromophore  $\alpha$  (decoupled from the remaining chromophores) and  $J_{v\mu}^{(\alpha\beta)}$  is the coupling strength between excitation  $v$  on chromophore  $\alpha$  and excitation  $\mu$  on chromophore  $\beta$ .  $J_{v\mu}^{(\alpha\beta)}$  is computed from

$$J_{v\mu}^{(\alpha\beta)} = \int d\mathbf{r}_1 d\mathbf{r}_2 \frac{\rho_v^{(\alpha)}(\mathbf{r}) \rho_\mu^{(\beta)}(\mathbf{r})}{|\mathbf{r}_1 - \mathbf{r}_2|}, \quad (2)$$

where

$$\rho_v^{(\alpha)}(\mathbf{r}) = \sum_{\substack{n \in \alpha \\ m \in \alpha}} \langle v^{(\alpha)} | c_n^\dagger c_m | g^{(\alpha)} \rangle \phi_n^*(\mathbf{r}) \phi_m(\mathbf{r}), \quad (3)$$

is the transition charge density associated with the  $v$ 'th excitation of group  $\alpha$ . Allowing the indices  $\mu v$  to run over the  $W$  and  $NV_1$  bands results in a model which accounts for coupling both within and between these bands, as was done in recent studies.<sup>8,10,13</sup>

Current Frenkel descriptions of polypeptide spectroscopy represent the transition charge densities of the constituent

amide groups using a small number of point monopole charges, *i.e.*<sup>1,8–10,14–16</sup>

$$\rho_v^{(\alpha)}(\mathbf{r}) = \sum_t q_{vt}^{(\alpha)} \delta(\mathbf{r} - \mathbf{r}_v^{(\alpha)t}), \quad (4)$$

so that the couplings  $J_{\mu\nu}^{(\alpha\beta)}$  are given by the Coulomb interaction of point monopoles,

$$J_{\mu\nu}^{(\alpha\beta)} = \sum_{\substack{t \in \alpha \\ s \in \beta}} \frac{q_{vt}^{(\alpha)} q_{\mu s}^{(\beta)}}{|\mathbf{r}_v^{(\alpha)t} - \mathbf{r}_{\mu s}^{(\beta)}|}. \quad (5)$$

Some theoretical studies of polypeptide absorption have obtained a monopole distribution using a quantum chemical computation of a molecule containing a single amide group.<sup>8–10,15,16</sup> Typically, these monopole charges have been reported without explicitly stating the Frenkel Hamiltonians obtained from them. For the sake of comparison with the current results, we have compiled in the Appendix three Hamiltonians used in past studies, two of which<sup>1,8</sup> have been reconstructed from the monopole distributions.

In the present study we will focus on the  $NV_1$  band and neglect its mixing with the much weaker  $W$  band. This mixing has been included in previous studies because it substantially augments the strength of the  $W$  band, which is not our concern here. We therefore use the single-band Frenkel Hamiltonian

$$H = \sum_{\alpha} \Omega_{\alpha} B_{\alpha}^{\dagger} B_{\alpha} + \sum_{\alpha \neq \beta} J_{\alpha\beta} B_{\alpha}^{\dagger} B_{\beta}, \quad (6)$$

where  $B_{\alpha}^{\dagger}$  creates an  $NV_1$  excitation on chromophore  $\alpha$ ,  $\Omega_{\alpha}$  is the energy of this excitation, and  $J_{\alpha\beta}$  is its coupling with the  $NV_1$  excitation on chromophore  $\beta$ .

### III. Computational method

To generate a polyaniline geometry, we first placed the heavy atoms according to the X-ray structure of Arnott and Wonacott.<sup>12</sup> Both ends of the chain were terminated with  $C_{\alpha}$ 's to reduce end effects, thereby providing a better model of a long chain. Subsequently, we optimized the locations of the hydrogens at the AM1 level.<sup>17</sup>

In Fig. 1 we introduce our numbering scheme for the heavy atoms and chromophoric groups of ALA5 (the extension of our numbering scheme to ALA15 is straightforward). As indicated in the figure, we refer to the direction along the polyaniline from the  $C_{\alpha}$  terminal which is bonded to a  $C'$  to the terminal  $C_{\alpha}$  which is bonded to an N as the chain direction.<sup>18</sup> We will refer to the opposite direction as the antichain direction. The division of the chain into chromophoric groups is also displayed in Fig. 1. We will address this issue in Section IV.

We have calculated the electronic excitations of  $\alpha$ -helical ALA5 and ALA15 using the CEO method.<sup>11</sup> The CEO method has previously been successfully applied to a wide variety of conjugated systems, including polyenes,<sup>19</sup> carotenoids,<sup>20</sup> phenylacetylene dendrimers,<sup>21</sup> naphthalene dimers<sup>22</sup> and the LH2 photosynthetic complex of *R. molischianum rho*-

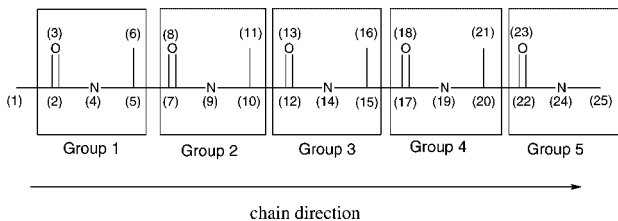


**Fig. 1** Numbering scheme for the heavy atoms and chromophores of ALA5  $CH_3-(CONHC_2H_4)_5-CH_3$ . The group indices start from  $k = 1$  and increase along the chain direction from the C to the N terminal. The indexing of the 15-amide polyaniline is analogous.

*dospirillum*.<sup>23</sup> To obtain the CEO, we begin with the second-quantized electronic Hamiltonian,<sup>24</sup>

$$H = \sum_{mns\sigma} t_{mn} c_{m\sigma}^{\dagger} c_{n\sigma} + \frac{1}{2} \sum_{\substack{ijmn \\ \sigma\sigma_1}} V_{ijmn} c_{i\sigma}^{\dagger} c_{j\sigma_1}^{\dagger} c_{n\sigma_1} c_{m\sigma}, \quad (7)$$

where the indices  $ijmn$  are summed over all electronic orbitals in the system, and  $\sigma\sigma_1$  denote the spin;  $t_{mn}$  is the single-electron matrix element, given by

$$t_{mn} = \int d\mathbf{r} \phi_m^*(\mathbf{r}) \left( -\frac{\hbar^2}{2m_e} + V_N(\mathbf{r}) \right) \phi_n(\mathbf{r}), \quad (8)$$

where  $V_N(\mathbf{r})$  is the nuclear potential, and

$$V_{ijmn} = e^2 \int d\mathbf{r}_1 d\mathbf{r}_2 \phi_i^*(\mathbf{r}_1) \phi_j^*(\mathbf{r}_2) \frac{1}{|\mathbf{r}_1 - \mathbf{r}_2|} \phi_m(\mathbf{r}_1) \phi_n(\mathbf{r}_2) \quad (9)$$

is the Coulomb interaction. In our study, we have used the semiempirical INDO/S<sup>25</sup> parameterization for  $V_{ijmn}$ .

To obtain the CEO equations, one begins with the Heisenberg equation of motion for the density operator  $\rho_{nm}^{\sigma} \equiv c_{m\sigma}^{\dagger} c_{n\sigma}$ ,

$$\frac{\partial \rho^{\sigma}}{\partial t} = i[H, \rho^{\sigma}]. \quad (10)$$

The CEO code computes the electronic excitations of the Hamiltonian (7) within the time-dependent Hartree-Fock (TDHF) approximation. The TDHF, which is equivalent to the random phase approximation (RPA), treats electronic correlations at an approximate level but with a considerably lower computational cost compared to *ab initio* calculations.<sup>19</sup> Using the assumption  $\rho^{\uparrow} = \rho^{\downarrow}$ , which allows us to drop the spin indices, we obtain

$$\frac{\partial \rho}{\partial t} = i[\rho, t + V(\rho)], \quad (11)$$

where the matrix elements of  $t$  were defined in eqn. (8), and

$$[V(\rho)]_{ms} = \sum_{nk} \rho_{kn} (2V_{nmks} - V_{nmks}). \quad (12)$$

To linearize (11), we take  $\rho = \bar{\rho} + \xi$ , where the ground state single-electron density matrix  $\bar{\rho}$  is the time-independent solution of (10), obtaining

$$i \frac{\partial \xi}{\partial t} = L\xi, \quad (13)$$

where the Liouville operator  $L$  is defined by

$$L\xi \equiv [t + V(\bar{\rho}), \xi] + [V(\xi), \bar{\rho}]. \quad (14)$$

The solutions of eqn. (13) are the normal modes  $\xi^v$ , which satisfy

$$L\xi^v = \Omega_v \xi^v, \quad (15)$$

where

$$\xi_{mn}^v = \langle g | c_{n\sigma}^{\dagger} c_{m\sigma} | v \rangle \quad (16)$$

is the transition density matrix, or electronic normal mode, for the transition between the ground state and the  $v$ 'th excited state. The  $\xi^v$ 's are normalized using their scalar product<sup>11</sup>

$$\text{Tr}[\bar{\rho}[\xi^{v\dagger}, \xi^{\mu}]] = \delta_{\mu v}. \quad (17)$$

The CEO code further provides a real space analysis for the electronic excitations and establishes a classical oscillator (quasiparticle) picture for collective electronic excitations in terms of  $\xi^v$  which can be viewed as *electronic normal modes*.

This makes it possible to pinpoint which parts of a complex multichromophore system contribute to a given electronic transition.

Below, we present excitation spectra and electronic normal modes computed using the CEO method. The normal modes directly show the roles of the various chromophores in the electronic excitations, and in particular reveal the importance of charge transfer between chromophores.

In the case of a molecular aggregate, CEO calculations performed on the uncoupled constituent chromophores can be used to construct a Frenkel Hamiltonian.<sup>26</sup> However, the applicability of Frenkel Hamiltonians to polypeptides is not

obvious due to the physical proximity of their chromophores. We have therefore used a modification of the formalism of ref. 26 to construct the Frenkel Hamiltonian for polyaniline. This construction, as well as its ability to describe the polyaniline excitation spectrum, will be discussed next.

#### IV. Excitation spectrum of the 5-amide polyaniline (ALA5)

The electronic normal modes of ALA5 are displayed in Fig. 2, and the associated oscillator strengths are listed in Table 1. In

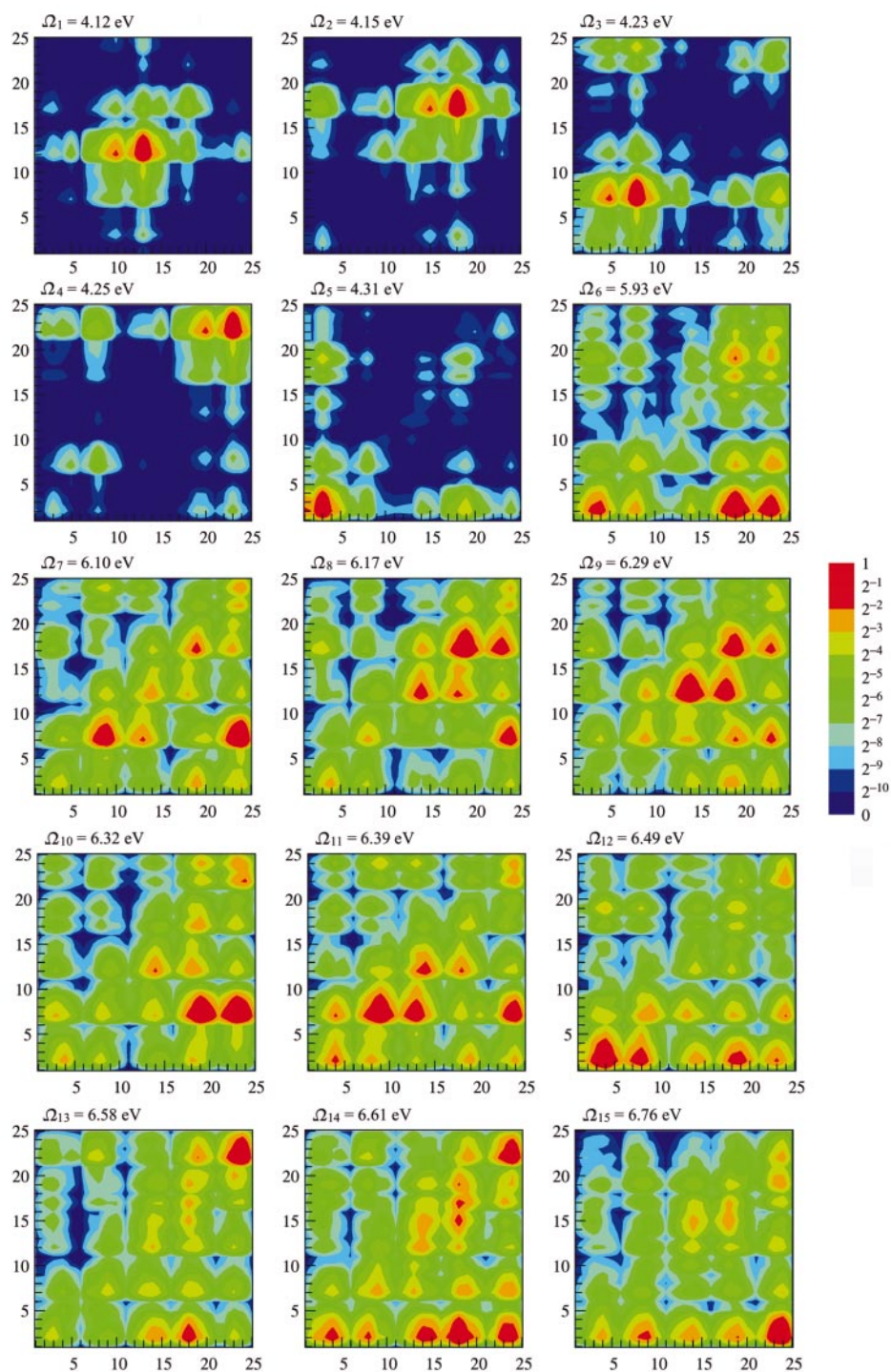


**Fig. 2** CEO modes of the  $\alpha$ -helical 5-amide polyaniline (log-2 scale). CEO modes 1–5 correspond to  $n\pi^*(W)$  transitions. Normal modes with substantial  $NV_1$  components occur between  $v = 6$  and  $v = 14$ , although some of these, especially  $v = 6, 7$  and  $10$ , are heavily mixed with charge-transfer transitions. Intrachromophoric (diagonal) components of these transitions are consistently associated with charge transfer from nearest-neighbor chromophores.  $v = 13$  and  $v = 15$  are almost entirely charge transfer transitions.

**Table 1** Oscillator strengths ( $f$ ) of excitations of the 5-amide polyalanine (ALA5).

$v$	1	2	3	4	5	6	7	8	9	10	11	12	13	14	15
$f$	0.04	0.04	0.07	0.05	0.07	0.72	3.75	2.47	1.72	0.14	1.92	1.27	3.16	1.16	0.24

these plots, point ( $a,b$ ) represents

$$K_{ab} = \sum_{\substack{n \in a \\ m \in b}} \xi_{nm}^2,$$

where  $nm$  are orbital indices and  $ab$  are atomic indices as enumerated in Fig. 1. A large value of  $K_{ab}$  indicates that the displayed mode involves the generation of electron-hole pairs with the hole on atom  $a$  and the electron on atom  $b$ . These plots have the appearance of a  $5 \times 5$  grid. Activity in diagonal (off-diagonal) blocks corresponds to transfer of charge within (between) amide groups. For example, the block located in the third column from the left and the second row from the bottom shows charge transfer from the third amide group to the second. The grid-like structure is highlighted by four dark vertical (horizontal) stripes whose horizontal (vertical) coordinates are 6, 11, 16 and 21, *i.e.*, the indices of the  $C_\beta$ 's. The evident lack of participation of the  $C_\beta$ 's in the  $NV_1$  excitations is not surprising considering their isolation from the  $\pi$  systems of the amide groups.

The structure of the CEO modes suggests a natural division of the polyalanine into chromophores, as shown in Fig. 1, which we will later use to construct a Frenkel Hamiltonian. Groups of heavy atoms which are separated in our indexing scheme by the  $C_\beta$ 's are taken to be independent chromophores. We then include the  $C_\beta$ 's in the same group as the  $C_\alpha$ 's to which they are bonded. Hydrogen atoms are included in the same groups as the heavy atoms to which they are bonded. In short, we include in each chromophore the three atoms C', N and O which form an amide group, the  $C_\alpha$  bonded to the N of that group, and the  $C_\beta$  bonded to this  $C_\alpha$ . This grouping of atoms is quite natural, and is ambiguous at most in that one could instead combine the amide group with the  $C_\alpha$  bonded to its C'. However, methylation of the amide-N to form *N*-methylformamide has been shown to have a much greater effect on the atomic excitation spectrum, and the  $NV_1$  transition in particular, than does the methylation of the C' to form acetamide.<sup>27,28</sup> This provides strong support for our scheme of dissecting the polypeptide into chromophores. We

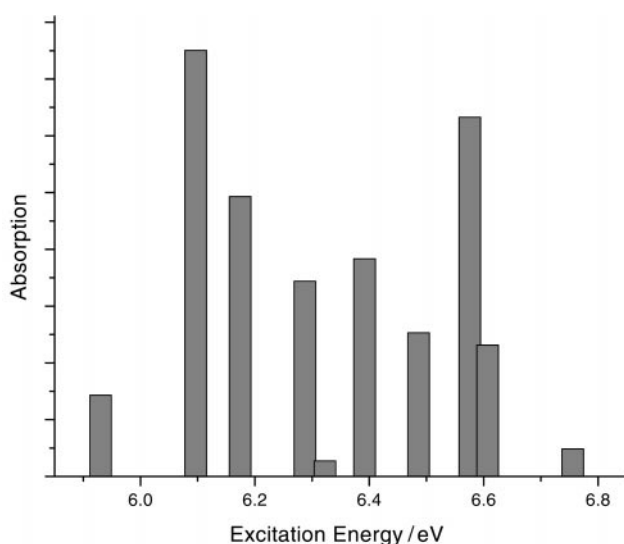


**Fig. 3** Linear absorption of the 5-amide polyalanine. For this short chain, the normal modes typically are most active at no more than one or two diagonal blocks. Consequently, the absorption strengths of the  $NV_1$  transitions are similar, although the 6.10 eV transition is arguably a precursor of Moffitt's longitudinal excitation.

number the groups starting from  $k = 1$  and increasing in the chain direction, as indicated in Fig. 1.

In the following examination of the CEO modes, it will be useful to quantify the interchromophore charge transfer which accompanies the excitations in the  $NV_1$  band. A convenient measure of the extent of charge transfer between chromophores is the quantity

$$Q_{\alpha\beta} = \sum_{\substack{n \in \alpha \\ m \in \beta}} \xi_{nm}^2, \quad (18)$$

where  $\sum_{n \in \alpha, m \in \beta}$  indicates a sum over normal mode components which transfer charge from atomic orbitals on chromophore  $\beta$  to atomic orbitals on chromophore  $\alpha$ . We will call this quantity the *charge-transfer strength*.

The five lowest-energy normal modes, which correspond to the  $n\pi^*$  (W) transition, vary in energy from 4.12 to 4.31 eV. This range substantially underestimates the experimental band center of 5.76 eV,<sup>29</sup> and is similar to previous redshifts of  $n\pi^*$  transitions by CI calculations using the CNDO/S Hamiltonian.<sup>30</sup> The  $NV_1$  band consists of normal modes  $v = 6$  through  $v = 14$ . According to standard exciton treatments of the  $NV_1$  band, we would expect that only the diagonal blocks should be active; that is, we would not expect to see charge transfer. However, each of these modes shows substantial activity in off-diagonal blocks. Indeed, a prominent feature of these plots is that the intrachromophoric (*i.e.* diagonal block) excitation of a group is nearly always accompanied by a transfer of charge onto that group from the nearest neighbor in the chain direction. In several of the transitions in this band, *i.e.*  $v = 6, 7$  and  $14$ , the dominant block of the normal mode is in fact a charge transfer component which has gained oscillator strength due to the weak mixing with an intrachromophoric transition. The identification of the intrachromophoric excitation as the source of oscillator strength follows from our present observation that normal modes without any significant diagonal component are always quite weak.

The  $v = 6$  transition consists of a  $\pi\pi^*$  excitation of the  $k = 1$  amide group, as well as electron transfer from  $k = 4$  and  $k = 5$  onto  $k = 1$ . In this instance, the charge transfer components are actually stronger than the diagonal component. According to the measure  $Q_{\alpha\beta}$  of charge transfer introduced earlier, the strengths of the dominant off-diagonal blocks in the  $v = 6$  mode relative to that of the dominant diagonal block (*i.e.*  $k = 1$ ) are  $Q_{14}/Q_{11} = 4.18$  and  $Q_{15}/Q_{11} = 1.98$ . Because the purely charge-transfer transitions tend to be weak, this transition most likely derives its oscillator strength from the relatively weak contribution of the diagonal component on the  $k = 1$  amide group. The  $v = 7$  transition consists mostly of an intrachromophore component on the second chromophore, and an electron transfer from the fifth chromophore to the second. Again, the off-diagonal charge transfer block is the most active, with  $Q_{25}/Q_{22} = 1.93$ . Similarly, the  $v = 14$  transition involves most dominantly a transition from  $k = 4$  to  $k = 1$ , and an intrachromophore excitation of  $k = 5$ . Since  $k = 5$  has no nearest neighbors in the chain direction (which are usually the charge donors during  $NV_1$  excitation), it does not involve significant charge transfer.

Except for  $v = 10$ , which is quite dominantly a charge transfer transition, and indeed has a small absorption strength, the most active blocks in the remaining transitions occur on the diagonal. Modes  $v = 8$  and  $v = 9$  are primarily

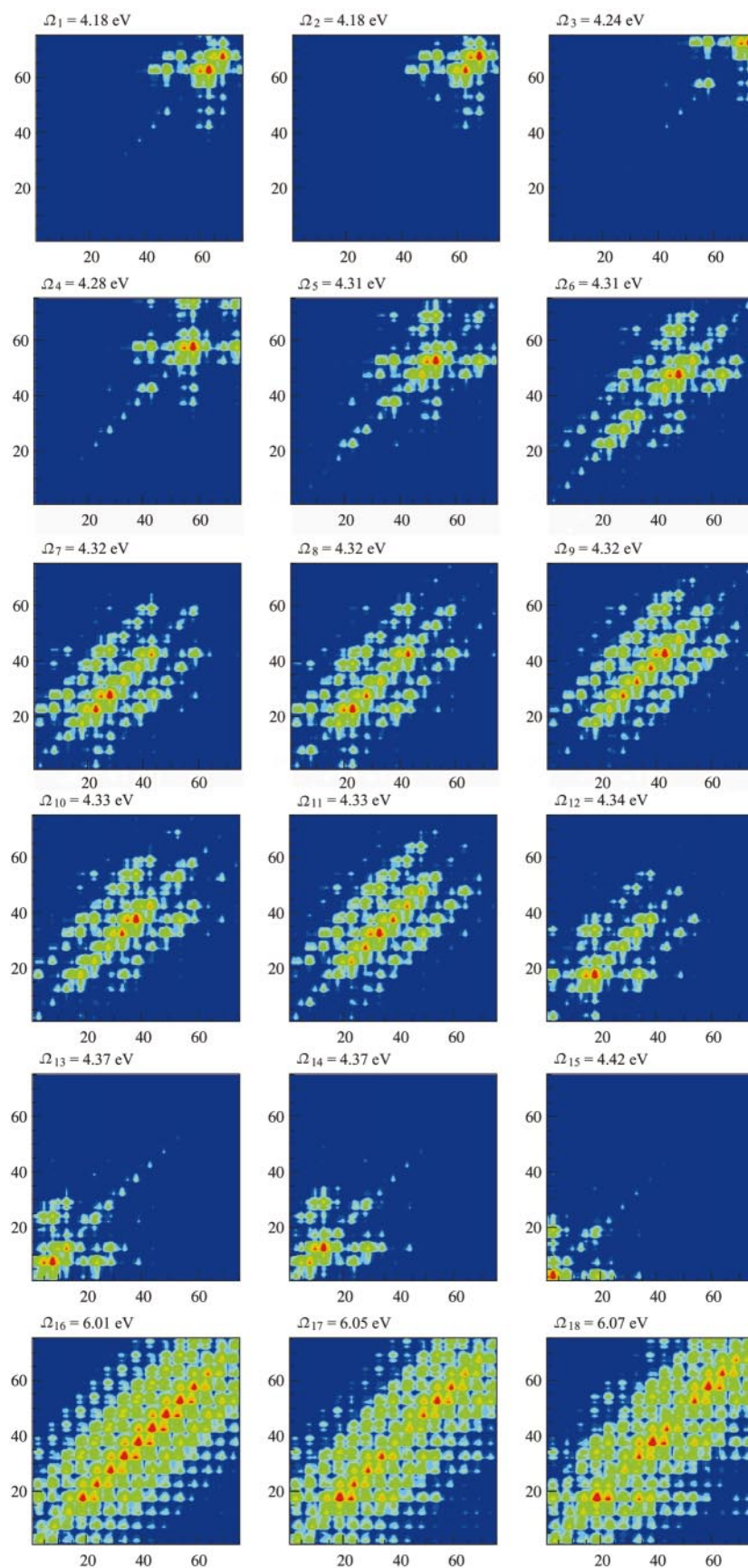


**Fig. 4A** CEO modes of the  $\alpha$ -helical 15-amide polyalanine. Large values on diagonal blocks indicate intrachromophore excitation, and large values on off-diagonal blocks indicate charge transfer. CEO modes 1–15 correspond to  $n\pi^*(W)$  transitions. Normal modes in the range  $v = 16$  through  $v = 32$  are dominated by the  $NV_1$  transition, with the exception of modes  $v = 24, 29$  and  $32$ , which are primarily charge transfer transitions.  $v = 16$  is the longitudinally polarized excitation predicted by Moffitt,<sup>1</sup> and the dominant transverse modes are  $v = 28$  and  $v = 31$ . An important feature of the  $NV_1$  transitions is that intrachromophore (diagonal) activity occurs in tandem with charge transfer from both nearest and third-nearest neighbours.

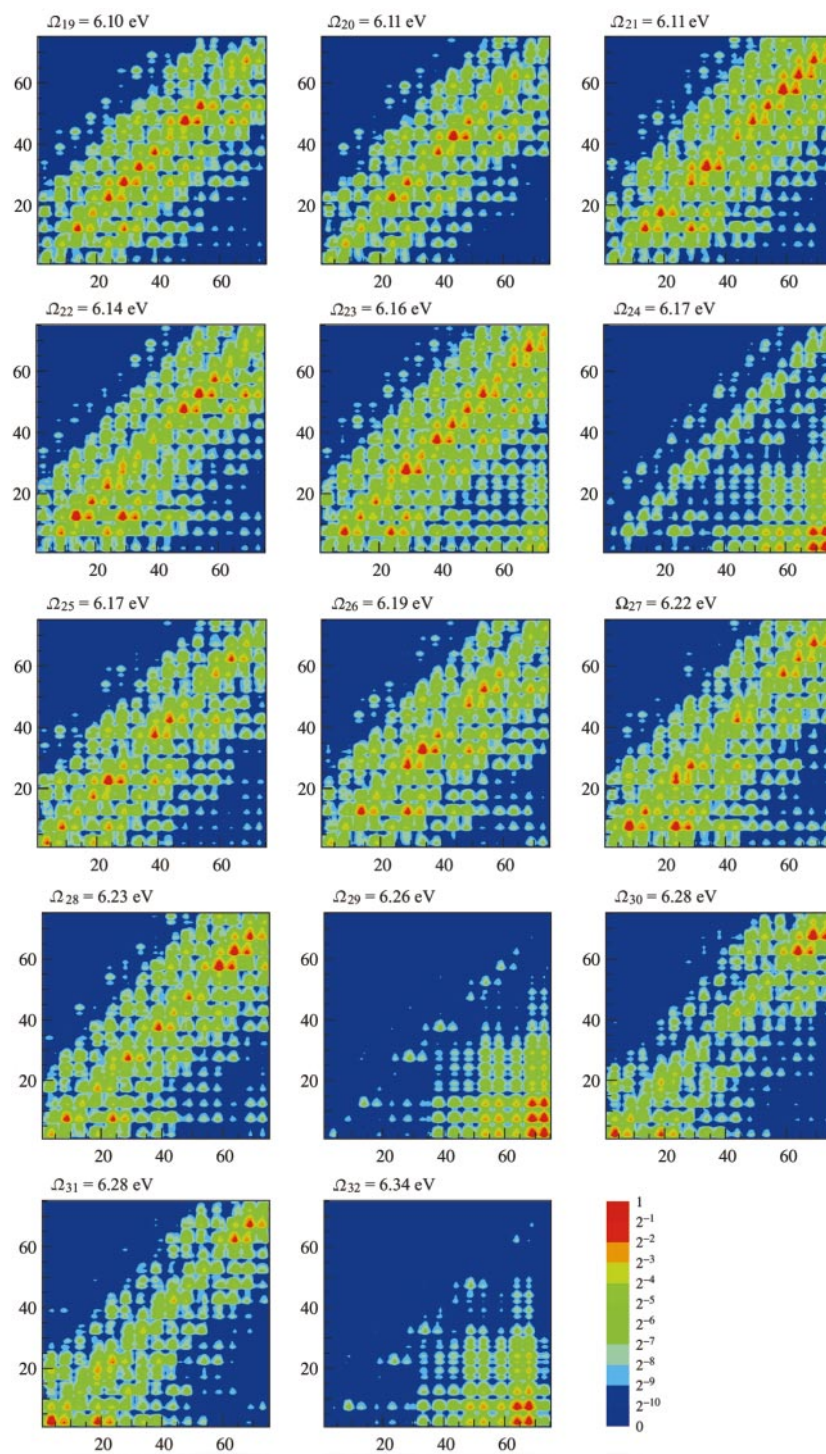


Fig. 4B Continued.

**Table 2** Oscillator strengths ( $f$ ) of excitations of the 15-amide polyaniline (ALA15)

$v$	$f$	$v$	$f$	$v$	$f$
1	0.04	12	0.06	23	2.05
2	0.05	13	0.06	24	0.04
3	0.06	14	0.03	25	2.30
4	0.08	15	0.04	26	3.04
5	0.09	16	16.19	27	1.04
6	0.14	17	0.20	28	9.07
7	0.07	18	0.96	29	0.00
8	0.20	19	0.65	30	2.26
9	0.02	20	0.43	31	6.72
10	0.04	21	0.21	32	0.00
11	0.16	22	1.69		

combinations of excitations on chromophores  $k = 3$  and  $k = 4$ , along with charge transfer from nearest neighbors in the chain direction onto these chromophores. The relative strengths of interchromophore to intrachromophore transition in these modes are, *e.g.*,  $Q_{45}/Q_{44} = 0.29$  in mode  $v = 8$ , and  $Q_{34}/Q_{33} = 0.47$  in mode  $v = 9$ . Modes  $v = 11$  and  $v = 12$ , although dominated by diagonal blocks, also involve transfers from nearest and third-nearest neighbors onto these dominant chromophores. In  $v = 11$ , the relative charge transfer strengths are  $Q_{23}/Q_{22} = 0.44$  and  $Q_{25}/Q_{22} = 0.42$ . In  $v = 12$ ,  $Q_{12}/Q_{11} = 0.28$ , and  $Q_{14}/Q_{11} = 0.24$ .

The linear absorption of ALA15 is presented in Fig. 3. Although it is tempting to identify the strongest transitions, at  $v = 7$  and  $v = 13$ , respectively as the longitudinal and trans-

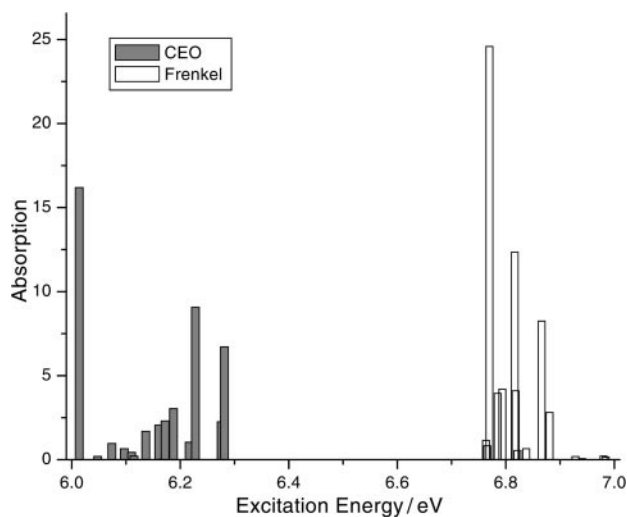


**Fig. 5** Linear absorption of ALA15 computed using both the CEO and Frenkel methods. The longitudinal absorption peak is at 6.01 eV, and the dominant transverse absorption peaks are at 6.23 and 6.28 eV. The linear absorption of the 15-amide polyalanine computed using a Frenkel Hamiltonian was obtained from a CEO calculation performed on a 5-amide polyalanine. The longitudinal absorption peak is at 6.77 eV, and the dominant transverse absorption peaks are at 6.82 and 6.86 eV. The Frenkel result for the longitudinal–transverse splitting is 67% less than the CEO result, and the longitudinal peak is blueshifted from the CEO result by 0.76 eV.

verse excitations predicted by Moffitt,<sup>1</sup> inspection of the corresponding plots provides only ambiguous support for this. In fact, the 5-amide chain is too short to meaningfully display the coherent superpositions of single-chromophore excitations

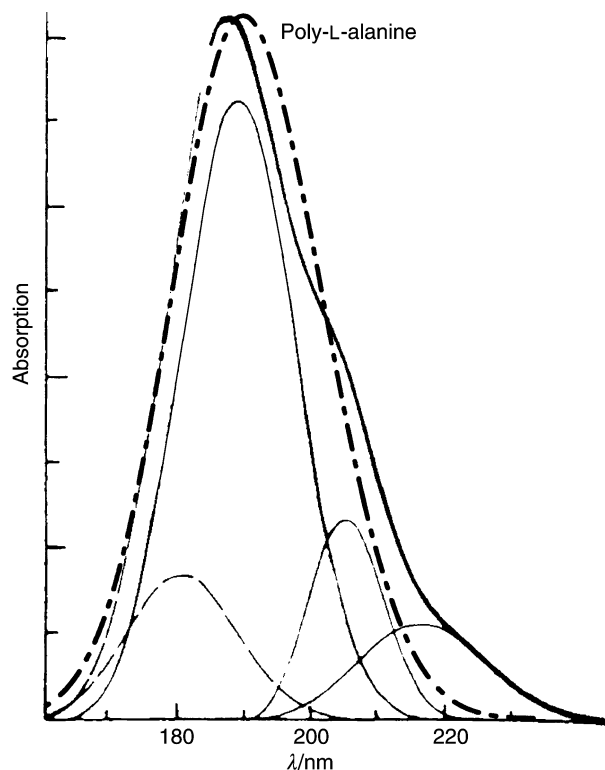


**Fig. 6** Heavy line: experimental linear absorption of polyalanine obtained by curve fitting the CD spectrum and demanding all spectral components have a positive sign. Dot-dash line: broadened absorption spectrum computed from the CEO. The lighter lines are a fit to the experimental absorption by four Gaussians. Based on this fit, the transverse  $NV_1$ , longitudinal  $NV_1$  and W bands were placed, respectively at 6.58 eV (204 nm), 6.10 eV (189 nm) and 5.76 eV (216 nm). An unidentified band is placed at 6.92 eV. Adapted from Quadrifoglio and Urry.<sup>29</sup>

which characterize these transitions, at least in the present computation. Consequently, we see that the absorption strengths of the various transitions in the  $NV_1$  band differ from each other by no more than a factor of  $\approx 2$ .

## V. Excitation spectrum of the 15-amide polyalanine (ALA15)

In this section we discuss the electronic excitations of  $\alpha$ -helical ALA15. The CEO modes of this molecule are displayed in Fig. 4, and the corresponding oscillator strengths are listed in Table 2. As in the case of ALA5, the  $n\pi^*$  transition frequencies computed for ALA15 are substantially lower than the experimental band center of 5.76 eV. Specifically, we find that the  $n\pi^*$  transitions span the energy range from 4.18 to 4.42 eV, with an absorption peak at 4.32 eV.  $v = 16$  is the lowest electronic normal mode belonging to the  $NV_1$  band and corresponds to the longitudinally polarized excitation predicted by Moffitt.<sup>1</sup> Inspection of this mode reveals a striking uniformity in the contribution of the participating chromophores, from  $k = 4$  to  $k = 12$ , as well as in the strengths of the charge transfer components. Charge transfer from nearest neighbors in both the chain and antichain directions is evident, as is charge transfer from third-nearest neighbors in both directions.

The next five transitions in the  $NV_1$  band are quite weak. The  $v = 17$  mode, like  $v = 16$ , has a fairly uniform appearance, but shows a modulation and a node at the center of the chain which are suggestive of the second harmonic of a vibrating string.  $v = 18$  has a similar structure with two regularly spaced modes. Of the remaining modes, only  $v = 23$  has both a comparable level of multichromophoric participation to the three lowest modes as well as a substantial oscillator strength. Modes  $v = 24, 29$  and  $32$  are nearly entirely of the charge transfer type, are spectroscopically weak, and are incidental to the  $NV_1$  band.

The CEO plots of the remaining transitions in the  $NV_1$  band show rather fractured patterns, with activity in isolated groups of between one and three chromophores. However, periodicities may be discerned upon close inspection. Modes  $v = 25$ – $28$  have an approximate four-chromophore periodicity which is close to the number of chromophores per turn in the present helix, which is 3.7. This is consistent with the behavior of the transverse polarized mode predicted by Moffitt,<sup>1</sup> in which the phase of the excitation cycles once per turn of the helix. We also notice that modes at the high energy end of the  $NV_1$  band tend to be most active at the ends of the molecule. This trend is particularly obvious with modes  $v = 30$  and  $v = 31$ .

One consistent feature shared by all of the modes in the  $NV_1$  band is the occurrence of interchromophore charge transfer in tandem with intrachromophore excitation. The plots show that intrachromophoric excitation, which appears as a feature on the diagonal blocks, is consistently associated with charge transfer onto the same chromophore from the nearest neighbor in the chain direction. A weaker charge transfer is associated with the nearest neighbor to the antichain direction. From the normal mode plots, we also see that the  $\pi\pi^*$  excitation of a particular chromophore  $k$  is also associated with charge transfer onto that chromophore from chromophore  $k + 3$ . This effect is quite reasonable due to the physical proximity and hydrogen bonding between third-nearest neighbors in  $\alpha$ -helices.

To provide representative numbers which characterize the charge transfer strengths for this band, we consider the  $v = 16$  mode, which, as we have noted, is highly uniform from one chromophore to the next in the strength of its charge transfer components. We find that for the seven chromophores nearest to the center of the molecule, from  $k = 5$  to  $k = 11$ , the average of the charge transfer strength from the nearest neighbor in the charge direction, relative to intrachromophoric exci-

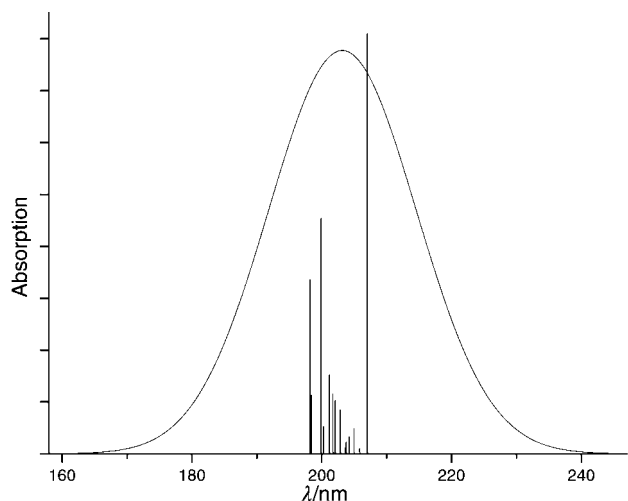


**Fig. 7** Absorption spectrum of the 15-amide polyalanine, computed by the CEO. The vertical lines are a bar-graph representation of the oscillator strengths listed in Table 2, and the smooth curve was obtained by convoluting this stick spectrum with a Gaussian of full-width half-maximum 25 nm.

tation strength, is  $\langle Q_{k, k+1}/Q_k \rangle = 0.221$ . Also, the relative strength of charge transfer from the nearest neighbor in the antichain direction is  $\langle Q_{k, k-1}/Q_k \rangle = 0.093$ . Finally, for third nearest neighbors in the chain and antichain directions, we have, respectively,  $\langle Q_{k, k-3}/Q_k \rangle = 0.024$  and  $\langle Q_{k, k+3}/Q_k \rangle = 0.027$ .

The linear absorption of ALA15 as calculated by the CEO is displayed as the filled bars in Fig. 5. This spectrum is dominated by three transitions, at 6.01, 6.23 and 6.28 eV, corresponding to modes  $v = 16, 28$  and  $31$ , respectively. As discussed above, inspection of the normal mode plots allows us to identify these modes as a longitudinal excitation ( $v = 16$ ), and two transverse excitations ( $v = 28, 31$ ).

In Fig. 6 we have reproduced the Quadrifoglio and Urry's<sup>29</sup> experimental linear absorption spectrum for polyalanine. The heavy solid line in this figure is an estimated spectrum based on experimental results, and the heavy dot-dash line is a fit based on the CEO stick spectrum of Fig. 5. To obtain this fit, we convoluted the stick spectrum with a Gaussian of full-width half-maximum 25 nm, producing the smooth curve shown in Fig. 7. By blueshifting this curve by 14 nm, thus moving the peak from 203 to 189 nm, we obtained the dot-dash curve of Fig. 6. The theoretical plot has the same general shape as the experimental trace, but does not reproduce the shoulder at 204 nm which is due to absorption by the longitudinal mode. The remaining traces in Fig. 6 are Quadrifoglio and Urry's decomposition of the experimental result into four Gaussians.

In this decomposition, bands associated with the longitudinal and transverse modes are placed, respectively, at 6.10 eV (204 nm) and 6.58 eV (189 nm). By comparison, the CEO computation places the longitudinal excitation at 6.01 eV and the transverse band center at  $\approx 6.30$  eV. The positions of these bands therefore compare quite reasonably with the experimental values. The more pertinent comparison, however, is the splitting between the bands, which, unlike the absolute positions, depends entirely on the interchromophore coupling. Our calculated splitting of 0.29 eV underestimates the experimental result<sup>29</sup> by 40%.

## VI. Analysis of the 15-amide polyalanine absorption using a Frenkel model

The coefficients  $J_{\alpha\beta}$  for the  $v$ th band of electronic excitations in a molecular aggregate may be related to the normal modes

via<sup>26</sup>

$$J_{\alpha\beta} = \sum_{\substack{n \in \alpha \\ m \in \beta}} V_{nmnm} \xi_{nn}^{v(\alpha)} \xi_{nm}^{v(\beta)}, \quad (19)$$

where  $\xi^{v(\alpha)}$  is the normal mode associated with the  $v$ th excitation on chromophore  $\alpha$ .<sup>26</sup>

The construction of a Frenkel Hamiltonian for polyanilines using eqn. (19) requires a set of normal modes  $\eta^\alpha$  which are localized on the respective chromophores. We have generated localized normal modes using a procedure in which the CEO eigen-mode associated with the excitation of a certain chromophore is projected onto the corresponding diagonal block. Given a normal mode  $\xi^v$ , a localized mode  $\eta^\alpha$  could be generated by defining the unnormalized projection operator

$$\tilde{\eta}^\alpha = \mathcal{P}^\alpha \xi^v \quad (20)$$

where

$$\mathcal{P}^\alpha \xi^v = \begin{cases} \xi_{nm}^v & n, m \in \alpha \\ 0 & \text{otherwise.} \end{cases} \quad (21)$$

A normalized local mode is then obtained from

$$\eta^{(\alpha)} = (\text{Tr}[\tilde{\rho}[\tilde{\eta}^{(\alpha)\dagger}, \tilde{\eta}^{(\alpha)}]])^{-1/2} \tilde{\eta}^{(\alpha)} \quad (22)$$

The prefactor in eqn. (22) assures that  $\eta^\alpha$  is normalized according to eqn. (17). Once we have generated one localized mode for each chromophore, the Frenkel couplings may be computed using

$$J_{\alpha\beta} = \sum_{\substack{n \in \alpha \\ m \in \beta}} V_{nmnm} \eta_{nn}^\alpha \eta_{nm}^\beta. \quad (23)$$

By inspection of the CEO eigen-modes given in Fig. 2, we have identified, for each chromophore of ALA5, the normal mode in the  $NV_1$  band for which the corresponding diagonal block is most active. Localized modes were then generated by the projection of the eigen-modes according to eqn. (21). This procedure gives us  $\tilde{\eta}^{(1)} = \mathcal{P}^{(1)} \xi^{12}$ ,  $\tilde{\eta}^{(2)} = \mathcal{P}^{(2)} \xi^{11}$ ,  $\tilde{\eta}^{(3)} = \mathcal{P}^{(3)} \xi^9$ ,  $\tilde{\eta}^{(4)} = \mathcal{P}^{(4)} \xi^8$  and  $\tilde{\eta}^{(5)} = \mathcal{P}^{(5)} \xi^{13}$ . After normalization of these localized modes according to eqn. (22), we may then use these modes to compute Frenkel couplings  $J_{\alpha\beta}$ .

Because the polyalanine geometries used in this study were generated from the geometry of a single residue using simple repetition of the internal coordinates, we expect that the couplings  $J_{\alpha\beta}$  should vary only weakly when  $|\alpha - \beta|$  is fixed. Therefore, a Frenkel Hamiltonian for ALA15 may be constructed by inserting the localized modes of ALA5 into eqn. (23). In doing so, we use the assumption that  $J_{\alpha\beta} \approx 0$  for  $|\alpha - \beta| > 4$ .

In summary, we have related the Frenkel couplings of ALA15 to those of ALA5 using the prescription:

$$J_{k, k+1} = \frac{1}{2}(J_{23} + J_{34}); \quad J_{k, k+2} = J_{24} \quad (24)$$

$$J_{k, k+3} = \frac{1}{2}(J_{14} + J_{25}); \quad J_{k, k+4} = J_{15} \quad (25)$$

The values of  $J_{\alpha\beta}$  on the right-hand sides of eqns. (24), (25) were taken from chromophores nearest the center of the polyalanine, where the end effects are weakest. For  $J_{k, k+1}$ , the couplings  $J_{23}$  and  $J_{34}$  are equally satisfactory under this criterion, so we have simply averaged their values, which are 0.0245 and 0.0259 eV, respectively. Likewise, for  $J_{k, k+3}$ , we have averaged  $J_{14}$  and  $J_{25}$ , which are  $-0.0461$  and  $-0.0500$  eV, respectively. These computations finally give us Frenkel couplings  $J_{k, k+1} = 0.0252$  eV,  $J_{k, k+2} = -0.0153$  eV,  $J_{k, k+3} = -0.0480$  eV and  $J_{k, k+4} = -0.0114$  eV.

To complete the specification of a Frenkel Hamiltonian we only need the single-chromophore energy and transition moment directions. These have been obtained from a CEO calculation of an *N*-methylacetamide molecule with the same heavy atom internal coordinates used for the generation of the



polyalanine geometries. The hydrogens were placed using an AM1 optimization. Application of the CEO to this structure found its  $NV_1$  transition energy to be 6.85 eV, and the transition moment direction to be  $\theta = -36.1^\circ$  where  $\theta$  is measured relative to the C–O bond direction, and  $\theta > 0$  is measured towards the direction of the C–N bond. Using these values, along with the  $J_{\alpha\beta}$  reported in the previous paragraph, we computed the absorption spectrum displayed as the open bars in Fig. 5.

It is useful to compare the absorption spectrum computed from the Frenkel Hamiltonian with the absorption spectrum obtained directly from the CEO, which are both displayed in Fig. 5. Both spectra are dominated by the three strongest absorption peaks. Interestingly, the two models find similar values for the heights of the three strongest peaks relative to each other. However, the positions of these peaks, 6.01, 6.23 and 6.28 eV in the CEO calculation, and 6.77, 6.82 and 6.86 eV in the Frenkel calculation, are very different. The discrepancy is properly viewed in comparison with the monomer transition of 6.85 eV computed for NMA. The CEO calculation finds that the lowest energy peak is redshifted from the monomer energy by 0.84 eV, with the other two peaks also substantially redshifted, by 0.62 and 0.57 eV. In the Frenkel calculation, the shifts are, respectively, redshifts of 0.08, 0.03 and a blueshift of 0.01 eV. The failure of the Frenkel model to account for the overall redshift of the absorption spectrum relative to the monomer is in fact quite common in Frenkel modeling of the  $NV_1$  absorption band.<sup>8,10,16</sup> Indeed, previous Frenkel parameterizations of this band<sup>8,10,16</sup> have assumed diagonal transition energies which are equal, or nearly equal, to the typical transverse absorption peak of 6.55 eV,  $\approx 0.3$  eV lower than the experimental NMA transition energy of 6.9 eV.<sup>31</sup> Our CEO plots suggest that this discrepancy may be due to a failure to account for charge transfer components inherent to the  $NV_1$  excitation.

Another important difference between the CEO and the Frenkel computation lies in the peak splittings. In the CEO, the difference between the highest- and lowest-energy of the three strongest peaks is 0.27 eV, which is three times the 0.09 eV splitting predicted by the Frenkel Hamiltonian.

## VII. Discussion

In this article we have tested the viability of the Frenkel model as a description of the electronic excitations of polypeptides. This was done by comparing the linear absorption computed from a Frenkel Hamiltonian for polyalanine with results obtained from direct calculations on a long polyalanine chain. Because the Frenkel couplings are extracted directly from computations on a multiple-segment chain, comparison of the Frenkel and full-molecule results provides a direct check of the internal consistency of the Frenkel model. Although our full molecule calculations are reasonably successful in determining the energies of the  $NV_1$  absorption peaks, as well as their redshifts relative to the monomer  $NV_1$  transition, the Frenkel model constructed from the multiple-segment results does quite poorly in these regards. The most critical point raised by the present Frenkel results are their inconsistency with the 15-peptide calculations. This failure, and its evident relation to the involvement of charge transfer in the electronic excitations, suggests an inherent limitation of the Frenkel approach which cannot be solved by higher level quantum chemistry calculations.

Only a handful of previous studies have considered the possibility of charge transfer excitations in amides. The Asher group used UV resonance Raman to experimentally demonstrate that the lowest allowed electronic transition in peptides is a charge transfer band from the penultimate carboxyl group to the adjacent amide bond.<sup>32</sup> A study of Serrano-Andrés and Fülischer<sup>33</sup> suggested, on the basis of dipeptide calculations,

that higher energy bands of polypeptides may be due to excitations which are predominantly charge transfer in character. A charge transfer transition has also been identified by Woody *et al.*,<sup>34</sup> who studied *N*-acetyl glycine using an INDO/S Hamiltonian at the CI-singles level. This study found a transition at 187 nm in which an electron is transferred from the  $\pi$  orbital of the amide group to the  $\pi^*$  orbital of the carboxyl group. However, prior studies did not explore the role of charge transfer in the  $NV_1$  band.

It is useful to consider possible extensions of the Frenkel model which would incorporate charge transfer effects. The most straightforward extension would be to introduce into the Hamiltonian an additional operator which is explicitly charge transfer in character, *i.e.*, which would create a hole on one chromophore and an electron on a neighboring chromophore. However, this would introduce degrees of freedom into the calculation which do not seem to be necessary to describe the  $NV_1$  band. For example, adding nearest-neighbor excitation operators to the Frenkel Hamiltonian would add 14 basis states to the single-excitation eigenspace in the case of the 15-amide polyalanine. However, the CEO results on this molecule show that there are only 15 transitions in the  $NV_1$  band with significant oscillator strength.

Another possible approach is to construct quasilocalized CEO modes following a procedure similar to eqns. (20)–(22). One could, for example, construct a quasilocalized electronic mode which has nonzero components associated with charge transfer within chromophore  $\alpha$ , and for charge transfer onto  $\alpha$  from chromophore  $\alpha + 1$ , all other components being zero. Using this approach, we found Frenkel couplings  $J_{\alpha\beta}$  which were highly sensitive to the choice of  $\alpha\beta$ , even for fixed  $|\alpha - \beta|$ . However, this method might be more reliable in conjunction with more sophisticated quantum chemistry.

Finally, we note that recent studies of Woody and Sreerama,<sup>8</sup> and Besley and Hirst<sup>10</sup> have reported methods capable of near-quantitative accuracy in the prediction of the CD strength of the  $NV_1$  band. The latter of these studies relies on *ab initio* calculations to parameterize the amide chromophore, and the former method uses a combination of experimental parameters in conjunction with parameters derived from configuration interaction calculations based on an INDO Hamiltonian.<sup>25</sup> We do not advocate the use of entirely semiempirical methods of the type described in this article as a quantitative alternative to any of these methods; however, we do hope that the results discussed here will provide some guidance for systematic study of charge transfer effects in the electronic spectroscopy of polypeptides.

## VIII. Acknowledgements

The support of the National Science Foundation and the Petroleum Research Fund administered by the American Chemical Society is gratefully acknowledged. We wish to thank Dr A. Piryatinski and Dr C. Scheurer for most stimulating discussions. S. A. A. gratefully acknowledges funding of this work by NIH grant GM30741.

## Appendix: polypeptide Hamiltonians

In this appendix, we summarize Frenkel couplings between  $NV_1$  transitions on different chromophores used in previous studies. In parts I and II, we have reconstructed these couplings from point charge distributions used in the earlier studies.

(I) In his seminal study of the  $NV_1$  band in  $\alpha$ -helical polypeptides,<sup>1</sup> Moffitt assumed that the transition charge density of an amide group could be modeled by placing a single point charge on each of its heavy centers, C', N and O. Within this model, the values of the point charges may be uniquely

**Table 3** NV<sub>1</sub> band couplings between amide groups in hemoglobin according to the Hamiltonian constructed by Woody and Sreerama,<sup>8</sup> the column headings  $\alpha$  and  $\beta$  refer to the index of the residue containing the carbonyl, as enumerated in PDB file 1HCO

$\alpha$	$\beta$	$J_{\alpha\beta}/\text{cm}^{-1}$	$\alpha$	$\beta$	$J_{\alpha\beta}/\text{cm}^{-1}$	$\alpha$	$\beta$	$J_{\alpha\beta}/\text{cm}^{-1}$
59	60	-593	62	63	-423	65	66	498
59	61	-655	62	64	-620	65	67	-673
59	62	-239	62	65	-74	65	68	-91
59	63	102	62	66	131	65	69	146
59	64	-68	62	67	-57	65	70	-62
60	61	45	63	64	378	66	67	-312
60	62	-595	63	65	-570	66	68	-628
60	63	-46	63	66	-137	66	69	-37
60	64	150	63	67	147	66	70	103
60	65	-52	63	68	-41	66	71	-18
61	62	390	64	65	-70	67	68	-58
61	63	-774	64	66	-644	67	69	-926
61	64	-81	64	67	-24	67	70	-106
61	65	128	64	68	120	67	71	66
61	66	-46	64	69	-49	67	72	-104

matched to an experimental transition moment using the relations

$$\mu = q_C r_C + q_O r_O + q_N r_N \quad (\text{A1})$$

$$0 = q_C + q_O + q_N \quad (\text{A2})$$

where  $r_i$  and  $q_i$  are the position and charge of center  $i$ . Moffitt obtained  $\mu$  from the experimental oscillator strength  $f = 0.237$ , the transition energy  $\nu = 54050 \text{ cm}^{-1}$ , and the experimental result that the transition moment direction makes a  $9.1^\circ$  angle with the line segment joining the N and O atoms.<sup>35</sup> These assumptions, along with the Pauling–Corey geometry of dihedral angles  $(\phi, \psi) = (-48^\circ, -57^\circ)$ , give the couplings  $J_{k,k+1} = 196 \text{ cm}^{-1}$ ,  $J_{k,k+2} = -468 \text{ cm}^{-1}$ ,  $J_{k,k+3} = -351 \text{ cm}^{-1}$ ,  $J_{k,k+4} = 49 \text{ cm}^{-1}$  and  $J_{k,k+5} = 49 \text{ cm}^{-1}$ .

(II) In a recent construction due to Woody and Sreerama,<sup>8</sup> the transition monopoles are chosen to coincide with a more recent experimental determination of the transition moment direction.<sup>36</sup> The transition monopole charges were not placed directly on the heavy centers, but rather at positions directly above and below, where the “above” and “below” directions are taken relative to the amide plane. More precisely, the monopoles were placed at the centroids of above-plane and below-plane transition charge densities, as determined from s and p orbital wavefunctions with semiempirically determined nuclear charges.<sup>37</sup> Woody and Sreerama applied this method to a set of representative protein structures from the Protein Data Bank (PDB). In Table 3 we have reconstructed the Hamiltonian so obtained for a 14-peptide hemoglobin segment extracted from residues 59–73 of PDB entry 1HCO.

(III) In the approach of Belsey and Hirst,<sup>10</sup> transition monopoles are determined from an *ab initio* study of *N*-methylacetamide. These monopoles are derived from multi-configurational second-order perturbation theory (CASPT2) based on a complete active space self-consistent field (CASSCF) reference state, and account for the environment using a self-consistent reaction field. The resulting electrostatic potential was approximated by placing five monopoles—a central charge and two dipoles near each of the heavy nucleus and the nuclei of the amide hydrogen (a total of 20 monopoles). They report that for an idealized helix, with dihedral angles  $(\phi, \psi) = (-57^\circ, -47^\circ)$ , the Frenkel couplings for the NV<sub>1</sub> band are  $J_{n,n+1} = -150 \text{ cm}^{-1}$ ,  $J_{n,n+2} = -640 \text{ cm}^{-1}$ ,  $J_{n,n+3} = -370 \text{ cm}^{-1}$  and  $J_{n,k} \approx 0$  for  $k > 3$ .

## References

- W. Moffitt, *J. Chem. Phys.*, 1956, **25**, 467; W. Moffitt, *Proc. Natl. Acad. Sci. U.S.A.*, 1956, **42**, 736; W. Moffitt and J. T. Yang, *Proc. Natl. Acad. Sci. U.S.A.*, 1956, **42**, 596.
- P. M. Bayley, E. B. Nielsen and J. A. Schellman, *J. Phys. Chem.*, 1969, **73**, 228.
- A. S. Davydov, *Theory of Molecular Excitons*, Plenum Press, New York, 1971.
- E. A. Silinsh and V. Capek, *Organic Molecular Crystals, Interaction, Localization and Transport Phenomena*, American Institute of Physics, New York, 1994.
- M. Pope and C. E. Swenberg, *Electronic Processes in Organic Crystals and Polymers*, Oxford University Press, NY, 1999.
- R. W. Woody, in *Circular Dichroism: Principles and Applications*, ed. K. Nakanishi, N. Berova and R. W. Woody, VCH Publishers, New York, 1994.
- R. W. Woody, in *Circular Dichroism and the Conformational Analysis of Biomolecules*, ed. G. D. Fasman, Plenum Press, New York, 1996.
- R. W. Woody and N. Sreerama, *J. Chem. Phys.*, 1999, **111**, 2844.
- J. D. Hirst, *J. Chem. Phys.*, 1998, **109**, 782.
- N. A. Besley and J. D. Hirst, *J. Am. Chem. Soc.*, 1999, **121**, 9636; J. D. Hirst and N. A. Besley, *J. Chem. Phys.*, 1999, **111**, 2846.
- V. Chernyak and S. Mukamel, *J. Chem. Phys.*, 1996, **104**, 444; S. Tretiak, V. Chernyak and S. Mukamel, *J. Chem. Phys.*, 1996, **105**, 8914.
- S. Arnott and A. J. Wonacott, *J. Mol. Biol.*, 1966, **21**, 371.
- The most general Frenkel Model contains additional coupling terms. Here we apply the Heitler–London approximation and only retain the dominant terms responsible for intermolecular energy transfer. For the most general Hamiltonian, see ref. 26.
- M. C. Manning, M. Illangasekare and R. W. Woody, *Biophys. Chem.*, 1988, **31**, 77.
- M. C. Manning and R. W. Woody, *Biopolymers*, 1991, **31**, 569, and references therein.
- G. Kurapkat, P. Krüger, A. Wollmer, J. Fleischhauer, B. Kramer, E. Zobel, A. Koslowski, H. Botterweck and R. W. Woody, *Biopolymers*, 1997, **41**, 267.
- M. J. S. Dewar, E. G. Zoebisch and E. F. Healy, *J. Am. Chem. Soc.*, 1985, **107**, 3902.
- G. E. Schulz and R. H. Schirmer, *Principles of Protein Structure*, Springer-Verlag, New York, 1979.
- E. V. Tsiper, V. Chernyak, S. Tretiak and S. Mukamel, *Chem. Phys. Lett.*, 1999, **302**, 77; S. Tretiak, V. Chernyak and S. Mukamel, *Chem. Phys. Lett.*, 1989, **287**, 75; V. Chernyak, M. Schulz, S. Mukamel, S. Tretiak and E. Tsiper, *J. Chem. Phys.*, 2000, **113**, 36.
- S. Tretiak, V. Chernyak and S. Mukamel, *Int. J. Quantum Chem.*, 1998, **70**, 711; S. Tretiak, V. Chernyak and S. Mukamel, *J. Am. Chem. Soc.*, 1997, **119**, 11408.
- S. Tretiak, V. Chernyak and S. Mukamel, *J. Phys. Chem. B*, 1998, **102**, 3310.
- S. Tretiak, W. M. Zhang, V. Chernyak and S. Mukamel, *Proc. Natl. Acad. Sci. U.S.A.*, 1999, **96**, 13003.
- S. Tretiak, C. Middleton, V. Chernyak and S. Mukamel, *J. Phys. Chem. B*, 2000, **104**, 9540; S. Tretiak, C. Middleton, V. Chernyak and S. Mukamel, *J. Phys. Chem. B*, 2000, **104**, 4519.
- A. Szabo and N. S. Ostlund, *Modern Quantum Chemistry*, Dover Publications, Mineola, NY, 1996.
- J. Ridley and M. C. Zerner, *Theor. Chim. Acta*, 1973, **32**, 111.
- T. Minami, S. Tretiak, V. Chernyak and S. Mukamel, *J. Lumin.*, 2000, **87–89**, 115.

- 27 L. Serrano-Andrés and M. P. Fülcher, *J. Am. Chem. Soc.*, 1996, **118**, 12190.
- 28 J. D. Hirst, D. M. Hirst and C. L. Brooks, *J. Phys. Chem. A*, 1997, **101**, 4821.
- 29 F. Quadrifoglio and D. W. Urry, *J. Am. Chem. Soc.*, 1968, **90**, 2755.
- 30 See ref. 15 and references therein.
- 31 K. Kaya and S. Nagakura, *Theor. Chim. Acta*, 1967, **7**, 117.
- 32 X. G. Chen, P. Li, J. S. W. Holtz, Z. Chi, V. Pajcini, S. A. Asher and L. A. Kelly, *J. Am. Chem. Soc.*, 1996, **118**, 9705; X. G. Chen, R. W. Bormett, S. J. Geib, P. Li, S. A. Asher and E. G. Lidiak, *J. Am. Chem. Soc.*, 1996, **118**, 9716.
- 33 L. Serrano-Andrés and M. P. Fülcher, *J. Am. Chem. Soc.*, 1998, **120**, 10912.
- 34 R. W. Woody, G. Raabe and J. Fleischauer, *J. Phys. Chem. B*, 1999, **103**, 8984.
- 35 D. L. Peterson and W. T. Simpson, *J. Am. Chem. Soc.*, 1955, **77**, 3929.
- 36 L. B. Clark, *J. Am. Chem. Soc.*, 1995, **117**, 7974.
- 37 R. W. Woody and I. Tinoco, Jr., *J. Chem. Phys.*, 1967, **46**, 4927.